

D. Keefe

Lawrence Berkeley Laboratory, University of California, Berkeley, California, USA.

Abstract

The current state of progress in experiments on ERA at Berkeley is reviewed. Experiments on high-current instabilities have been in progress for several months with the newly constructed high-current electron accelerator. The major experimental and theoretical attack at present is addressed to understanding the stabilization of the negative-mass instability, which is limiting the ring quality. Stable rings with 6×10^{12} electrons have been formed but with a larger energy spread than desired.

A. Introduction

At the VIIIth International Conference on High Energy Accelerators at Yerevan, I described the experiments then in progress with a device we called Compressor 3 which operated in conjunction with the Astron electron accelerator at Livermore¹⁾. Efforts to extract the ring and accelerate it axially in a magnetic solenoid led only to a slow spill-out of the electrons without preservation of the integrity of the ring as a compact structure²⁾. Detailed measurements of the properties of the rings formed in that experiment showed them to be uniformly of poorer quality (measured in terms of holding power) by an order of magnitude than those we had previously formed and studied in an earlier experiment (Compressor 2) at Livermore.³⁾ With diffuse dimensions and too few electrons the failure of the ring to accelerate as an integral unit was understandable because ion-focussing and image-cylinder focussing could not maintain axial focussing of the ring during extraction. Fig. 1 shows an example of the dividing line between the ranges of electron number (N_e) and minor dimensions (a,b) that determine whether a certain ion-loading can maintain axial focussing or not; rings formed in Compressor 2 would have been adequate, those in Compressor 3 were not. The formation of high quality rings in that experiment was thwarted by a combination of single-particle and collective effects difficult to disentangle; the major culprit was the negative-mass instability, which caused tight azimuthal bunching of the beam with large radial spreading and loss of particles.²⁾ We still have no definitive explanation of why these two compressors behaved so differently, but it is presumably because of differences in the electrical environment.

In the following year we built our own high-current electron injector at Berkeley to allow continuing experiments to be made. Having been once hurt badly by collective instabilities we determined to study these phenomena thoroughly with a ring-forming apparatus called Compressor 4. Construction was also begun on a new device to accelerate ions, Compressor 5, and this is now almost complete.

Begun first at 2 MeV these experiments have been in progress for almost a year, apart from an interruption of a few months to raise the injector energy to 4 MeV.

B. The Electron Injector

The electron injector commenced useful operation at 2 MeV one year ago⁴⁾. In Spring 1971 the final units were added to bring the energy to 4 MeV. The basic accelerating module is an (untuned) cavity that contains an accelerating gap (5 cm across) and a torus of ferrite (40 cm in diameter). Connected to the cavity is an oil-filled Blumlein line 4 meters long that constitutes the driving pulse-shaping circuit and energy storage. The Blumlein line is charged from a Marx generator to 250 kV and is discharged by a triggered spark-gap. In terms of a low-frequency analogy, the rate of rise of flux in the ferrite due to the driving pulse leads to an accelerating potential of 250 kV across the gap. The energy per gap delivered to the beam is somewhat less than this because of a partially-terminating network and because of beam loading. The general configuration of the accelerator consists of one accelerating cavity and one solenoid lens at one-meter intervals. The gun section is an exception in that five cavities are bolted together and are threaded by a stainless-steel rod, the end of which is a high-voltage terminal accumulating the 1.25 MV sum of the five cavities.

We gambled on developing a successful cold-cathode source of long-life and relatively low jitter. The design did not preclude use of a hot cathode, but the three, or so, orders of magnitude to be gained in current density from a cold emitter made the gamble seem worth-while.

The present cold cathode is a 0.0005 in. tantalum ribbon wound in a spiral of several turns. Emission occurs at the ribbon edge. This type of cathode has been successful and its lifetime for jitter-free operation is several months.

Typically the injector is run at one pulse every 2 or 3 seconds and delivers a 900A pulse about 25ns long on the flat-topped voltage pulse. The accelerator has been run at a repetition rate greater than 1 Hz and, by modifying the charging supplies, could go to 10 Hz, but so far this mode of operation has not been needed. The two-dimensional transverse emittance is about $\pi(.08)$ cm rad which exceeds the compressor acceptance ($\pi \times 0.05$). A set of variable-thickness foils allow introduction of energy-spread of known amounts with some loss in beam current. A set of screens can be introduced to attenuate the beam-current without modifying the emittance. The transport line to the compressor contains a chopper to select a pulse of desired length - typically the pulse lengths used have been 4 ns or 16 ns, corresponding respectively to one-turn or four turns in the compressor.

* Work supported by the U.S. Atomic Energy Commission

We feel confident that the brightness of the injector can be increased. At present, however, our limitations have been due to collective instabilities in the compressor and we have not worked yet towards optimizing the injector brightness.

C. Compressor IV

The equipment that has been used for experiments in recent months is called Compressor 4 and is shown in cross-section in Fig. 2. It was intended to be limited in the sense that only two, rather than three, stages of compression are provided, but flexible so that geometric modifications and changes to the interior, can be made fairly rapidly. The probes used for non-destructive (magnetic loops, microwave detectors) and destructive (obstacle probes) diagnosis of the rings have been described earlier²⁾. The operating pressure is typically 1 or 2×10^{-6} Torr.

The injected beam enters at a radius, R , of 21 cm and is stacked on a closed orbit radius of 18 cm. Most of the experiments have used a one-turn (4 ns) beam because the diagnosis of the behavior of successive turns in the early stages of beam capture is much easier than with multi-turn injection. While useful for diagnostic purposes, it must be noted that one-turn injection is not to be favored for operation because it involves a rather violent initial condition on the modulation of the beam.

D. Observations and Interpretations

- a) Betatron Resonances: Because we choose to inject with a magnetic field index gradient, $n = -\frac{r}{B_z} \frac{\partial B_z}{\partial r}$, close to 0.5, and approach $n = 0$ at the end of compression, a variety of potentially dangerous resonances (n -value = 0.5, 0.36, etc.) have to be crossed. In setting up any of the compressor experiments we have been careful to minimize the field perturbations - mainly from the injection snout - that drive these resonances. Nevertheless we have usually found it essential to add small programmed correcting currents in the various compression coils to ensure that passage across certain resonances is rapid and amplitude growth thus prevented. The choice of the timing and magnitude of these currents has been greatly facilitated by use of a computer code NUERA, developed by L.J. Laslett and B.S. Levine which allows the calculation of the fields and their derivatives, including complicated eddy current effects, to a high degree of accuracy.
- b) Gas Instability: On occasion, when setting up an experiment with Compressor 4 before it had been pumped down to its usual operating pressure, we observed a radial beam instability corresponding to the lowest precessional mode $(1-\nu_R)f_0$. The time of onset, t , of this radial transverse coherent oscillation was rather precisely correlated with the pressure, P , of the background gas (see Fig. 3) such that $Pt = 10^{-3}$ Torr- μ sec. Similar behavior was observed when hydrogen and later nitrogen were admitted to the compressor. These results were useful in experimentally determining the ratio of ionization rates in different gases, and in verifying that the background base-pressure gas was

nitrogen-like; the latter is important to know for estimating the ion-loading from the background gas in the compressor.

The time of onset of this instability corresponded approximately to total neutralization of the ring ($N_i/N_e \approx 1$). Several types of gas instability have been discussed in the literature. We did not, however, pursue observations sufficiently to identify the nature of the instability since it is in a pressure range many orders of magnitude above what is needed for realistic ion-acceleration experiments.

c) Transverse Coherent Instability (Resistive-Wall):

Under good vacuum conditions it was observed that at a level of $N_e \approx 5 \times 10^{11}$, a strong transverse coherent radial instability occurred in the lowest mode, describable as a precessional motion of the ring as a whole with a frequency, equal to $(1-\nu_R)f_0$. This instability showed up quite clearly as the development of a large coherent radial amplitude, and analysis of the corresponding r-f bursts associated with this behavior showed a dominant frequency, $(1-\nu_R)f_0$. The threshold was observed to move to higher intensities when the side plates were made of lower resistance, as predicted from understanding of the resistive-wall driving term. As the intensity of the beam was increased above threshold, the onset of the instability and beam loss occurred earlier in time.

The threshold should be shifted to a higher value by an increase in the Landau damping that arises from the spread, ΔS , in the quantity $S = (1-\nu_R)f_0$, viz.,

$$\Delta S = \frac{\partial S}{\partial E} \Delta E + \frac{\partial S}{\partial a^2} \Delta a^2,$$

where E is the electron energy and "a" is the radial betatron amplitude. The coefficients of the differentials depend on the n -value and $\frac{\partial n}{\partial r}$; the second term on the right hand side is rather small in Compressor 4. There were two puzzling features about the experimental observations. First, the threshold current and time of onset of the instability were found to be essentially unaffected by increasing the injected beam energy spread from $\Delta E/E < 0.5\%$ to $\Delta E/E \approx 2\%$. Second, there was the observation in the early Compressor 2 experiment³⁾ of ring currents an order of magnitude higher without any evidence of this instability, and yet the locations of Coil Sets 1 and 2 in the old and present compressors were the same.

The suggestion made by Sessler⁵⁾ that a zero in the coefficient $\frac{\partial S}{\partial E}$ could lead to a virtually undamped situation independent of ΔE proved to be correct. A careful examination by Laslett of the structure and magnitude of the $\frac{\partial S}{\partial E}$ term showed⁶⁾ that indeed this coefficient came very close to zero about 20 μ sec after injection (Curve a, Fig. 4). The sharp drop in $\frac{\partial S}{\partial E}$ at that time was largely due to an unfriendly contribution to $\frac{\partial n}{\partial r}$ from eddy-

currents in Coil Set 2. Further computation for the geometry of the coils in Compressor 2, led to a resolution of the second puzzle, illustrated by Curve c (Fig. 4) which shows that the $\frac{\partial S}{\partial E}$ term did not in that case come very close to zero. While Coil 2 there produced unfriendly contributions to $\frac{\partial n}{\partial r}$ because of eddy currents, these were nullified by eddy-current contributions favorable in sign due to the presence of Coil Set 3 in that experiment and absent in the current compressor!

Further computation for Compressor 4 showed that replacement of Coil Set 2 by stranded conductor (which would have negligible eddy-current effects) would lead to behavior of $\frac{\partial S}{\partial E}$ shown in Curve b (Fig. 4). When this physical change was made, the transverse instability became no longer limiting, presumably because the threshold had been shifted to a substantially higher value because of Landau damping. At how high a current level this instability will again cause trouble is not yet known.

It would be noted that the Landau damping coefficient can be controlled by manipulation of both n and $\partial n / \partial r$. An extra degree of control can be gained by introduction of an azimuthal magnetic field produced by an axial current. This technique will be described in a paper at this conference by Laslett and Schumacher⁽⁷⁾.

d) Longitudinal Instability (Negative Mass): For the past several months we have been engaged in detailed studies - still continuing - of the negative mass instability, in which strong self bunching of the beam into one or more azimuthal bunches occurs. This may take place rapidly in a few turns and is accompanied by strong energy spreading, and consequent increase in the radial minor dimension of the ring and loss of holding power. If it happens near injection then, in addition, beam loss occurs because those particles shifted upwards in energy will be lost by scraping on the injection septum.

One method for increasing the threshold, N_e , for the negative-mass instability is to increase the frequency spread in the beam (Landau damping) through momentum spread. The Landau damping coefficient $\Delta\Omega/\Delta E$ is essentially proportional to $(1-n)^{-1}$, and unlike the case of the transverse instability we are not free to vary it by changing parameters other than the n -value, such as derivatives of n , or by introduction of axial currents. Introduction of momentum spreads larger than 2% are undesirable for forming rings of compact minor dimensions. We have successfully formed rings with $N_e = 6 \times 10^{12}$, with long term survival, but only with considerable spread in momentum.

Another method for stabilizing the beam is to surround it with a suitable electrical environment. A succinct way of describing the stabilizing action of the surroundings is in terms of the "coupling impedance" of the beam, viz.,

$$Z_n = - \frac{2\pi R E_n}{I_n}$$

where E_n, I_n are the amplitudes of the n^{th} harmonic of the field and current in the beam. Then Z_n is essentially the bunching voltage per turn per ampere of modulation and if it can be kept small enough a high current beam can be stabilized. This condition can be written approximately

$$\left| \frac{Z_n}{n} \right| \lesssim \frac{mc^2 \gamma}{e I_0} \left(\frac{1}{1-n} \right) \left(\frac{\Delta E}{E} \right)^2$$

(In principle Z_n can exceed this limit provided it is almost purely inductive). In general Z_n contains contributions from four sources; (i) a self-field term, (ii) a term due to the distributed impedance of the neighboring wall, (iii) a term due to lumped impedances, (iv) a term due to the finite radius of curvature of the ring.

At this point let me point out two features of our experiments that are different from the case of synchrotrons or storage rings - apart from the obvious fact that we are dealing with much lower energies and higher currents. First, the topology of the compressor is not that of a donut surrounding the beam cross section, but rather resembles a pill-box. Furthermore, typical distances, e.g. from the beam to an image surface or to a diagnostic probe, or the beam minor dimension, are not very small compared with the major radius of the beam. (For example, curvature contributions to Z_n are substantial.) Second, in our configuration, the conductivity of the side walls or circumferential band are limited because both the pulsed guide field and the pulsed inflector field (rise-time ≈ 20 ns) must penetrate and lead to insignificant eddy-current effects. A wall to stabilize the instability should have a low impedance at the cyclotron frequency (260 MHz), but must have high impedance at 10-20 MHz to be satisfactory for injection, thus constraining us to a rather narrow window of choice.

A considerable amount of theoretical effort has taken place in the last year to determine the effects of different types of surroundings with the aim of treating more realistically the actual conditions and limitations of our compressor. These and studies made in earlier work are briefly summarized in Table I. Most are limiting cases in certain of the variables, but have shed light on the effects and phenomena to be expected e.g. pill-box resonance, dielectric resonances, etc. A case of greater applicability, i.e. a pill-box having walls with an arbitrary μ, ϵ and σ , is the subject of a computer program now nearing completion by A. A. Garren and S. J. Sackett.

Hand in hand with the purely theoretical attack, has been the development of an electrical system for directly measuring the beam coupling impedance by simulating the beam with an electrical conductor. Three types of measurements - pulse response, standing-wave, and travelling-wave phase-shift - are made and the different contributions to Z_n can be isolated. The realities of complicated structures and lumped impedances - not very amenable to theoretical treatment - are directly measured by this method. This work, by Falten, et al, will appear in the Proceedings of this Conference⁽⁸⁾. Although superficially similar to techniques used to estimate

Table I

Calculations of negative mass coupling impedance

Beam	Model Walls	Required for $ Z /n < 40 \Omega$	Radiation and /or Resonances?	Reference
Straight	Laminated Tube	$Z_s \lesssim 10\Omega/\square$ diameter $2b \approx 10$ cm	Dielectric resonances	A. B.
Straight	Tube with given wall impedance	Avoid lumped wall impedance	Lumped elements resonating	C.
Cylindrical (E-) layer	Infinitely conducting tube	$\frac{b}{R} \lesssim 1.1$	Tube modes	D. E.
Ring	Infinitely conducting tube	$\frac{b}{R} \lesssim 1.1$	Tube modes	F.
Ring	Tube of given "Q-value"	$\frac{b}{R} \lesssim 1.25$ at $Q = 10$ $\frac{b}{R} \lesssim 1.15$ at $Q = 100$	Tube modes	G.
Ring	Pill box	$Q \lesssim 10$	Cavity modes	H.
Ring	Infinite, plane side-walls, infinitely conducting	$\frac{W}{R} \lesssim 0.2$	"Coherent radiation"	I.
Ring	Infinite plane laminated side-walls, arbitrary σ, ϵ, μ .	$Z_s \leq 4\Omega/\square$ $W/R \lesssim 0.2$	"Coherent radiation"	J.
Ring	Free space	$ Z /n \approx 300 \Omega$	"Coherent radiation"	L. K.

References:

- A) B. Zotter: CERN-ISR-TH/69-35
- B) A. Garren: ERAN-136 (1971)
- C) A. Sessler, V. Vaccaro: CERN 67-2
- D) R. Briggs, K. Neil: Plasma Phys. 9 (1967) p. 209
- E) I.N. Ivanov: JINR Preprint, P9-3476-2 (1967)
- F) R. Briggs: (ERA/WC-8)
- G) A. Garren, D. Mohl, in preparation
- H) A. Entis, L. Smith: ERAN-100 (1970)
- I) B. Zotter: CERN-ISR-TH 170-54
- J) C. Pellegrini, A. Sessler: (ERA/WC-22)
- K) A. Garren, A. Entis, D. Mohl, in preparation
- L) A.G. Bonch-Osmolovski, et al.: JINR Preprint P-9 5622 Dubna 1971

Z_s = surface impedance of wall (ohms/square). R = beam major radius T = 4 MeV
 b = tube radius W = distance from sidewalls

the coupling impedance in sections of the ISR beam pipe the authors believe the method to be novel and more general and to have important application to measuring existing accelerators.

Studies with the electron ring beam have proved more time-consuming than expected. Some of the parameters that have been tested are shown in Table II.

Table II

Parameter	Range
$\gamma (= E/mc^2)$	4.6, 8.5
$\Delta E/E$	< 1/2%, 1%, 2%, 4%
I (injected current)	2A to 250A
ohms/square: Outer band	few ohms to ∞
ohms/square: Sidewalls	4, 20, 50, ∞ (dielectric)
Distance to wall (w)	5 - 15 cm

The main diagnostic tools used were magnetic pick-up loops that either show the bunching of the beam or, when integrated, the circulating current as a function of time. A variety of pick-up loops are used to span the range of sensitivity and frequency response to study rapid losses (~ 10 nsec) or slow losses (100 μ sec). In addition movable obstacle probes are used to measure the minor dimensions of the beam as a function of time. Microwave detectors

are used to measure higher harmonics of the cyclotron frequency L band for $n \geq 4$, X-band for $n \geq 30$. Single-turn injection was used for most experiments to facilitate following the progress of the beam turn by turn in the early stages. Multi-turn injection which leads to a smoother, less lumpy beam in general gave higher circulating currents and higher thresholds for the instability.

Some examples of the type of data we are accumulating are shown in Fig. 5. At low currents the circulating current that persists is proportional to the injected current, but a saturation occurs at high currents. At about the same current level the radial width increases rather sharply in many cases as if a satellite of lower energy was developed. These current levels also correspond to a threshold in microwave activity.

At the lowest currents the r-f activity is small and, as the current is increased, one observes a developing growth (in tens of turns) of modulation at f_0 , at higher current a more rapid growth at f_0 followed by the onset of higher harmonics, and, at the highest current levels, very rapid onset of f_0 and many higher mode numbers (nf_0). As the injected current is increased, rf activity appears successively at higher harmonics, without any indication of some particular mode being preferentially excited.

These observations are hard to relate with the "thresholds" calculated from linear theory, and should be viewed in terms of a phenomenological change in behavior leading to deterioration in beam quality at high currents. In that sense we have found that the "damage threshold" is increased

roughly in proportion to γ . It does not vary as $(\Delta E/E)^2$ but more slowly, possibly as $(\Delta E/E)$. This can be understood in terms of the instability growing at a lower threshold, with small amplitude, developing energy-spread in the process and then becoming stable. Since it is the final state of the beam we observed not much effect on the radial width will be apparent until $\Delta E/E$ has grown to exceed 2%.

Although theoretical considerations suggest stabilization for close sidewalls with $R \lesssim 4\Omega/\text{square}$ we have not been able satisfactorily to explore this region. Penetration of the inflector field requires $R \gtrsim 2-4\Omega/\text{square}$, but we have only recently been able to make walls which are in this range. Many experiments have been attempted with sideplates in this conductivity range made by plating on a Kapton backing either gold, or gold-nichrome laminations, or nichrome or by etching stainless steel foil. None of these sidewalls survived the deposition of charge or the currents arising from the inflector field for a long enough time to make useful measurements. After many frustrations we have abandoned thin-metal film plating or etching and are now exploiting a variety of other techniques. These include making concentric metal rings broken in several places and capacitatively re-connected, deposited carbon or ferrite layers, and networks of many resistors. We feel we must verify the effectiveness of the sidewalls in this resistance range and still have compatible inflection, and, in addition, develop a durable fabrication method before

proceeding to ion acceleration experiments in Compressor 5.

It should be re-iterated that use of a single-turn provides a rather harsh condition, but it is the one we have continued to use to test in a consistent way the differences in electrical environment. A few experiments have been done by injecting a multi-turn beam and quite respectable surviving rings with $N_e \approx 6 \times 10^{12}$ electrons have been observed even with walls of poor conductivity.

References

1. D.Keefe, Proceedings VIIth International Conf. on Particle Accelerators, Yerevan, Armenia (Aug. 1969), Vol. II, p. 447.
2. D.Keefe, W.W.Chupp, A.A.Garren, G.R.Lambertson, L.J.Laslett, A.U.Luccio, W.A.Perkins, J.M. Peterson, J.B. Rechen and A.M.Sessler, Nucl. Instr. & Methods, 93, 541 (1971).
3. D.Keefe, G.R.Lambertson, L.J.Laslett, W.A. Perkins, J.M.Peterson, A.M.Sessler, R.W.Allison, W.W.Chupp, A.U.Luccio and J.B.Rechen, Phys. Rev. Letters, 22, 558, (1969).
4. R.Avery, G.Behrsing, W.W.Chupp, A.Faltens, E.C. Hartwig, H.P.Hernandez, J.Macdonald, J.R. Meneghetti, R.G.Nemetz, W.Popenuck, W.Salsig and D.Vanecek, Proceedings Accelerator Conf. (March 1971) IEEE Trans. on Nucl. Sci., NS-18, 3, p. 479 (1971).
5. A.M. Sessler, Private Communication (1970).
6. L.J. Laslett, "Arithmetic Pertaining to Landau Damping for Compressor 4", LRL Report ERAN-121, Dec. 1970, unpublished.
7. L.J.Laslett and U.Schumacher, paper to be presented at this conference.
8. A.M. Sessler, IEEE Trans. on Nucl. Sci., NS-18, p. 1039 (1971).
9. A.Faltens, E.C.Hartwig, D.Mohl and A.M.Sessler, paper to be presented at this conference.

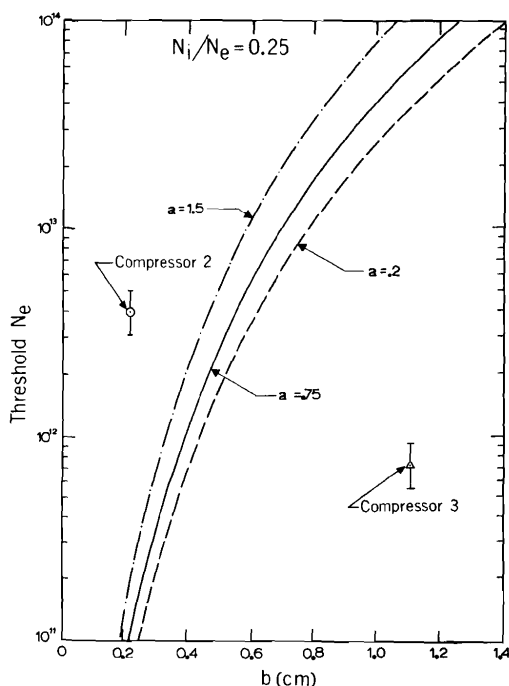
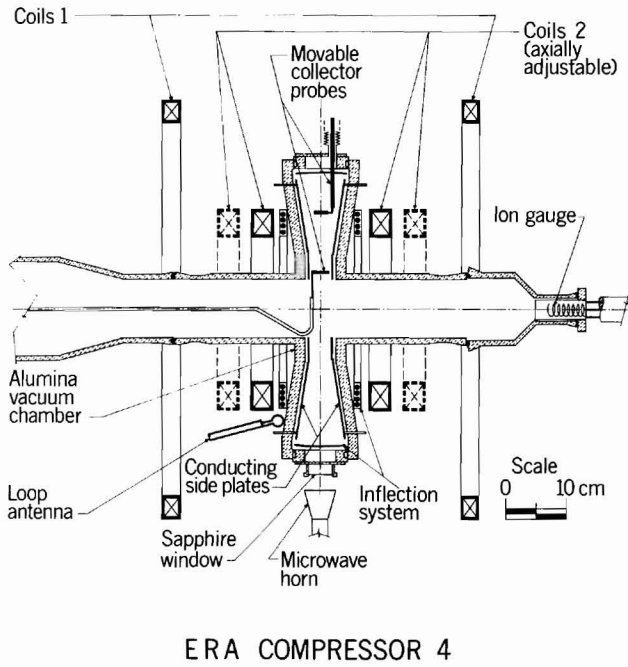


Figure 1 - The threshold number of electrons, N_e , versus the ring minor axial dimension, b , required for axial stability for an ion fraction $N_i/N_e = 0.25$. The result does not depend very strongly on the minor radial dimension a .

DISCUSSION

- R. WILDERÖE : How long was your total compression time ?
- D. KEEFE : Each coil has a quarter period of about 250 μ s. Thus, for three stages of compression, the total time would be about 750 μ s.
- B. ZOTTER : Have the frequencies of the microwave instabilities been measured and could they be identified with specific pill-box or dielectric-wall resonances ?
- D. KEEFE : We have not observed specific pill-box or dielectric-wall resonances. The frequencies observed are all attributable to the cyclotron frequency and its harmonic.



ERA COMPRESSOR 4

Figure 2 - Cross-sectional view of Compressor 4.

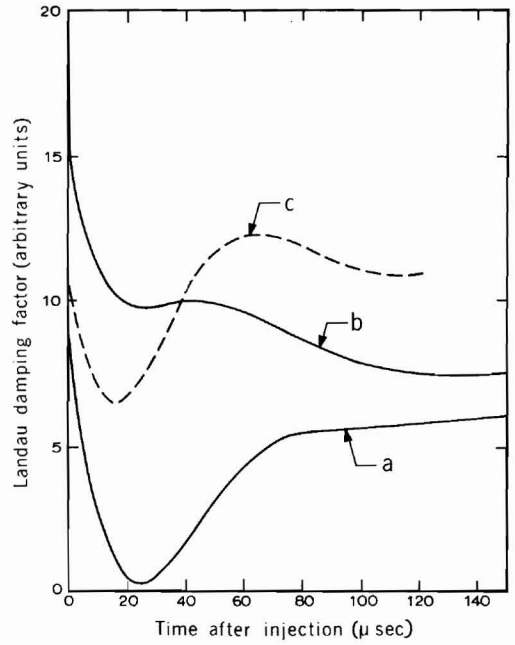


Figure 4 - Landau damping coefficient versus time for a) Compressor 4 (solid copper coils), b) Compressor 4 (stranded coils), c) Compressor 2.

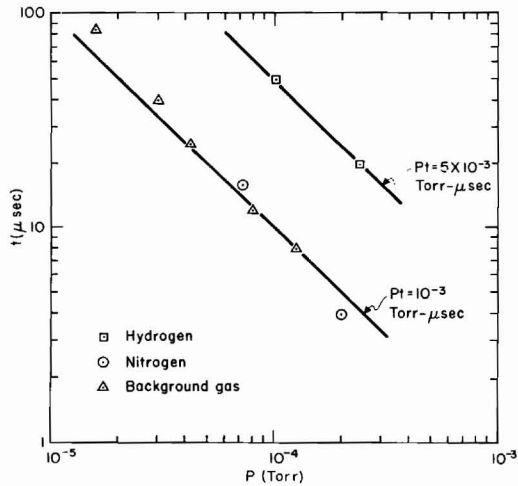


Figure 3 - The relation between gas pressure and the time of onset of the gas-induced precessional instability.

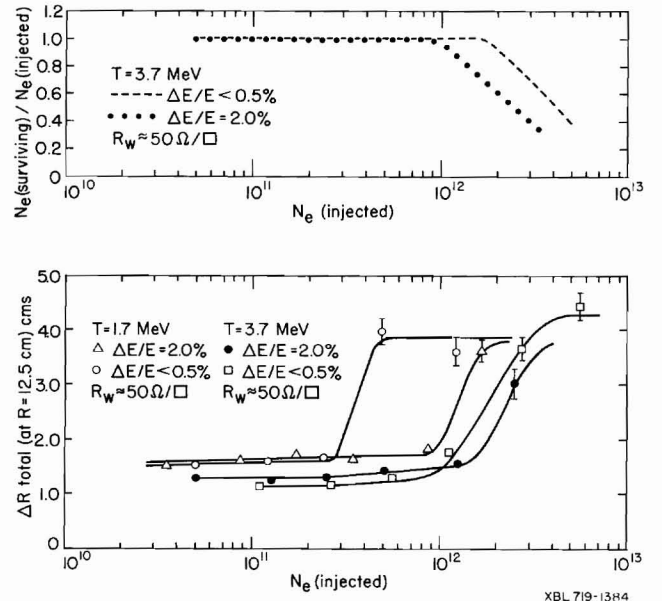


Figure 5 - Circulating current and maximum radial width of the ring at $R = 12.5$ cm as functions of intensity.

XBL 719-13R4